Plant Physiol. (1992) 100, 1869–1877
0032-0889/92/100/1869/09/$01.00/0

Received for publication January 13, 1992
Accepted July 20, 1992

Energy Storage of Linear and Cyclic Electron Flows in Photosynthesis[1]

Yuan Cha[2] and David C. Mauzerall*

The Rockefeller University, New York, New York 10021

ABSTRACT

The energy storage of photosynthesis in the green alga *Chlorella vulgaris* was determined by pulsed, time-resolved photoacoustics. The energy storage of the linear electron transfer process in photosynthesis, of cyclic photosystem (PS) I, and possibly of PSII was determined by selection of excitation wavelength and of flash interval. At 695 nm excitation, a rather large cyclic PSI energy storage of 0.68 ± 0.04 eV/quantum of energy at 8 ms after a 1-μs flash was obtained. This energy remained the same at flash intervals of 0.35 to 60 s and was independent of the presence of 3-(3,4-dichlorophenyl)-1,1-dimethylurea. We tentatively assign this energy to the ferredoxin-NADP-reductase-ferredoxin and oxidized cytochrome b_6/f complexes. An efficient distribution of energy between cyclic and linear systems is obtained with the simple assumption that the turnover time of the cyclic system is slower than that of the linear system. The energy storage of linear electron flow was determined by 655 nm excitation of *Chlorella* with a short flash interval of 0.35 s per flash. It was calculated to be 0.50 ± 0.03 eV/hv, close to that expected for oxygen and NADPH formation. The energy storage of PSII is determined by excitation of *Chlorella* at 655 nm with a long flash interval of 60 s per flash. It was calculated to be 1.07 ± 0.05 eV/hv, consistent with the energy storage being in S-states and the secondary electron acceptor of PSII with a calculated redox energy of 1.03 eV/hv. In the presence of 1 μM 3-(3,4-dichlorophenyl)-1,1-dimethylurea, the calculated energy storage in PSII is still significant, 0.53 ± 0.04 eV/hv. This probably indicates a significant cyclic electron flow around PSII. These cyclic flows may contribute considerably to energy storage in photosynthesis.

The technique of photoacoustics has been applied to photosynthetic systems for some time (10, 26, 30) with a variety of useful results, including the direct measurement of O_2 formation in intact leaves (8, 11, 28). A unique application of photoacoustics is to determine the TE[3] of photosynthesis, i.e. the ratio of energy stored in the system, following an appropriate delay, to the energy of the absorbed light. The photoacoustic methodology allows an astonishingly simple, fast, and accurate measurement of this value. Several workers (9, 13, 20, 26) have applied modulated light photoacoustics to study energy storage at approximately 10 ms. The advantage of pulsed, time-resolved photoacoustic methodology is its more direct connection to the kinetics of thermal changes (28). The energy storage will begin at 100% (the trap energy, approximately 1.8 eV in green systems) and decrease stepwise through the photosynthetic chain of reactions to that of the final products, roughly O_2 and sugars, with a TE of approximately 30%.

Because these reactions occur on different time scales, in principle, the TE for each reaction can be determined by time-resolved photoacoustics. Specifically, the photoacoustic methodology measures the enthalpy of the time-resolved step(s) of the reaction. The difference between these measured enthalpies of reaction and the standard free energy calculated from known values gives information concerning concentration ratios of reactants and other entropic contributions to the system.

In this work, we have applied pulsed, time-resolved photoacoustics to determine the energy storage over the range of 2 to 20 ms following a 1-μs laser pulse to intact cells of *Chlorella vulgaris*. The energy storage in intermediates that are formed faster than within 2 ms and that decay slower than within 20 ms is determined. By selection of excitation wavelength, we have determined the TE for linear electron flow through PSII to PSI and that for cyclic electron flow in PSI and possibly in PSII. The energy storage in PSII and in PSI were determined by varying flash intervals and by use of inhibitors.

MATERIALS AND METHODS

Photoacoustic Apparatus

The pulsed, time-resolved photoacoustic system begins with a 1-μs dye laser (Candela dye laser model LFDL-2). The 695-nm light was obtained by oxazine 720 (40 μM in CH_3OH) and the 655-nm light by sulforhodamine 640 (80 μM in CH_3OH) (Exciton dyes). The laser light passed through a refractive attenuator (Newport Corp. model 935-5) and a heat filter of a solution of transition metal ions and was focused onto one branch of a bifurcated fiber optic bundle. The homogenized laser light from the fiberoptic bundle was directed onto a photoacoustic cell. The second branch of the fiberoptic bundle was coupled to a power meter (Laser Precision model Rj-7200), and the scattered light from the sample was collected to monitor the variation of pulsed light energy. The continuous background light (Cole-Parmer model 9741-

[1] This work was supported by the National Science Foundation grant DMB 87-18078.

[2] Present address: Merck Research Laboratory, P.O. Box 2000, Rahway, NJ 07065.

[3] Abbreviations: TE, thermal efficiency; CCCP, carbonyl cyanide *m*-chlorophenylhydrazone; Cyt b_6/f, cytochrome b_6/f complex; DBMIB, dibromothymoquinone; FNR, Fd-NADP-reductase; Q_A and Q_B, primary and secondary electron acceptors of PSII.

50) was focused onto the sample from the side. The photoacoustic signal was detected by a microphone (Knowles model BL-1785) whose output was amplified 10- to 1000-fold (Ithaco 1201 low noise preamplifier) with low- and high-pass filters set between 1 Hz and 10 kHz. The output was connected to a digitizer (Keithley 194A high-speed voltmeter), and the data were transferred to and analyzed by a computer (Hewlett-Packard model 320). All programs were written by the authors.

The photoacoustic cell was described previously (28). Two identical photoacoustic cells were used in these experiments in differential form to help cancel the background noise from the surroundings. An air-floating table was used to reduce the vibrations (Newport Stable Top). The signal from the microphone is the time differential of the pressure change and is integrated following digitization to obtain the desired pressure (28). We used wet black paper as a standard sample to check the linearity of the acoustic signal and found it to be so from 10^{13} to 10^{15} quanta cm^{-2} $pulse^{-1}$ with a correlation coefficient of 0.997. This standard also showed an energy storage of $0 \pm 2\%$.

The flash energy was delivered onto the sample of area 1.1 cm^2. Below approximately 10^{13} quanta cm^{-2} $pulse^{-1}$, the signal to noise ratio was too low to give a reliable measurement. Each photoacoustic trace was the result of an average of 20 flashes with flash intervals of 0.35 or 60 s in the dark. We refer to these as fast and slow flash rates. The acoustic measurements in the presence of background saturation light are always at the fast flash rate to minimize sample heating. With a flash number greater than 64, the TE decreases. This effect is probably caused by overheating the sample in the presence of saturating background light for extended times.

Algae

Batch cultures of the green alga *Chlorella vulgaris* were grown at 20°C in continuous light from cool-white fluorescent lamps (19). The light intensity was 130 μE m^{-2} s^{-1} (Biospherical Instruments, San Diego, CA, model QSL-100 light meter). We used 3- to 5-d-old cells for our experiments. A final concentration of 0.1 M $NaHCO_3$ was added to the growth media before filtration, and the cells were filtered onto a support (Millipore membrane filter 8.0 μm, 1.3 cm diameter) that was then placed into the photoacoustic cell. Changing the concentration of $NaHCO_3$ had no effect on TE. Occasionally, the cells on the filter paper were resuspended into media and counted. The sample comprised two to three layers of *Chlorella* (average cell diameter 5 μm). For the DCMU-inhibited sample, 1 μM DCMU final concentration was added to the growth media before filtration. The same procedure was carried out with other inhibitors.

Control Experiment

An experiment was carried out to determine the effect of optical thickness of samples on TE. We found that the signal to noise ratio was too low to make accurate measurement when the sample was less than two layers of *Chlorella*. The TE remained the same ($<\pm 2\%$) when the sample comprised more than two to three layers of *Chlorella*. Theoretical calculation was also carried out to determine the effect of optical thickness of samples on TE. The effect was less than 1%.

An experiment was carried out to determine the contribution of O_2 to the acoustic signal in the case of the algal sample. No O_2 was detectable photoacoustically ($\pm 2\%$) with *Chlorella* samples at the fast flash frequency, in contrast to results with intact leaves. This was due to the thick water layer in the algal samples. The amount of water in the *Chlorella* sample was determined by weighing, and the water layer was calculated to be approximately 60 μm thick. The time for an O_2 molecule diffusion to the surface is estimated to be a few seconds, too slow to be detected by our microphone. At the slow flash rate, no O_2 signal was observed even for leaves, presumably because of loss of the S-states.

The TE of *Chlorella* was determined as a function of flash interval in the presence and the absence of DCMU at 655 nm. With flash energy of 2.5×10^{13} quanta cm^{-2} $pulse^{-1}$, the TE was constant (about 20%) from 0.1 to 3 s per flash and then increased to about 29% at 60 s per flash. With 695 nm excitation, the TE does not change over this range of flash intervals.

Theory

Calculation of Energy Storage

At the time of a photoacoustic measurement following a μs pulse of light to the photosynthetic system otherwise in the dark, the absorbed photon energy (E_{lt}) can be divided into four parts. First, the energy of each absorbed photon above the photosynthetic trap energy (E_o approximately 690 nm or 1.8 eV) is immediately degraded to heat. Second, a small fraction of the trap energy is emitted as fluorescence (E_f^d). Third, a fraction of this energy is degraded to heat in steps previous to the measurement. Both this heat and the prompt excess energy heat are included in the measured heat (E_h^d). Finally, there is the energy stored in various ways by the photosynthetic system at the measuring time (E_p^d). The first factor simply rescales the total energy absorbed by the system:

$$E_{lt} = E_o\, \upsilon_{lt}/\upsilon_o \quad (1)$$

where υ_{lt} and υ_o are the frequency of the absorbed photon and that corresponding to the trap energy, E_o, respectively. In the dark, E_{lt} is composed of three fractions:

$$E_{lt} = E_f^d + E_h^d + E_p^d \quad (2)$$

In the presence of continuous saturating background light in which reaction centers are closed, the absorbed pulsed photon energy is emitted as fluorescence (E_f^l with an increased yield over E_f^d) and dissipated as heat (E_h^l):

$$E_{lt} = E_f^l + E_h^l \quad (3)$$

The TE is defined as the ratio of chemical energy of

photosynthesis to the total absorbed light energy. By definition and Equation 2,

$$TE = E_p^d/E_{lt} = (E_{lt} - E_f^d - E_h^d)/E_{lt} = 1 - Y_f^d - E_h^d/E_{lt} \quad (4a)$$

because

$$E_f^{d,l} = Y_f^{d,l} \cdot E_{lt}.$$

Using Equation 3,

$$TE = 1 - Y_f^d - (1 - Y_f^l)\, E_h^d/E_h^l \quad (4b)$$

In Equation 4, a and b, $E_h^d = \alpha H^d$ and $E_h^l = \alpha H^l$, where H^d and H^l are the acoustic signals at a given time following a flash to the sample in the dark and in the presence of saturating continuous light, respectively. The factor α is an instrumental constant. $Y_f^{d,l}$ are the fluorescence energy yields in the dark and saturating continuous light. As shown in Equation 4b, one simply measures the heat liberated at a given time by photoacoustics in the dark and in the presence of background light. If the fluorescence yields are known, the TE is obtained.

Correction for Fluorescence Yield

For finite flash energy, one should include a correction to the previous equations due to the partial (or even complete) closure of reaction centers during the flash time, and hence, an increase of the fluorescence yield. E_f^d and, therefore, Y_f^d are actually a function of flash energy. The fluorescence yield at different flash energies is calculated by Equation 5, which allows for the change in yield on the second and greater hits to a unit via the Poisson distribution (27):

$$Y_f^d = \frac{(Y_f^{do} - Y_f^l)\,(1 - e^{-\sigma_2 E})}{\sigma_2 E} + Y_f^l. \quad (5)$$

In Equation 5, Y_f^{do} is the fluorescence energy yield when the reaction centers are fully open, Y_f^l is the fluorescence energy yield when the reaction centers are closed, σ_2 is the optical cross-section of PSII in cm^2 (24), and E is the flash energy in quanta cm^{-2} $pulse^{-1}$. The cross-section of PSII is used because the increase in fluorescence yield is essentially all from this photosystem. $Y_f^{d,l} = (v_o/v_{lt})\,\phi_f^{d,l}$, where $\phi_f^{d,l}$ are the absolute quantum yields of fluorescence in the dark and in the light, respectively. The mean frequency of fluorescence is assumed to be equal to the trap frequency, v_o. For *Chlorella*, the quantum yields in the dark and in saturating light have been determined to be 2.7% (23) and 8.1% (25), respectively.

Analysis of TE as a Summation of Linear and Cyclic Electron Flows

There are two ways to divide the TE of photosynthesis on this 2- to 20-ms time scale. The first, applicable to intact systems, is to divide the TE into that from linear electron flow and that from a cyclic electron flow. Experimentally, this is achieved by excitation with a "short" flash interval of 0.35 s per flash. The second, applicable to inhibited or isolated systems, is to divide the TE into that from PSII and that from PSI. This is achieved by excitation with a "long" flash interval of 60 s per flash or, alternatively, by use of inhibitors. The "long" flash interval generates the charge-separated species in PSII, S_2- and S_3-states and Q_B^-, whose lifetimes are longer than the measuring time of 2 to 20 ms but shorter than the time between hits to the reaction centers, approximately 300 s for the lowest flash energy used. DCMU inhibits electron flow from PSII to PSI, and thus the two systems are isolated. We will use both of these analyses on our data where applicable.

The relation between linear and cyclic electron flow is still poorly understood. However, there is a simple mechanism for a maximal TE. If PSI cycled when it did not receive an electron from PSII after a certain time of being "hit," TE would be optimized. Thus, a simple assumption, that the turnover time of cyclic electron flow is greater than that of linear flow, is sufficient to ensure a high TE without need of a control system. Because the maximum turnover time of the linear system is about 10 ms when the plastoquinone pool is reduced (29), the maximum turnover time of the cyclic system would have to be somewhat slower.

Because the linear electron flow from H_2O to $NADP^+$ requires a 1:1 ratio of PSI to PSII, using the above assumption the TE can be written as a sum of cumulative one-hit Poisson saturation functions (Eq. 6) (25). The observed TE is the summation over that for linear electron flow and that for cyclic electron flow and divided by the total number of photons absorbed.

$$TE = \frac{2TE_{lin}N_2\,(1 - e^{-\sigma_2 E}) + TE_c\,(N_1[1 - e^{-\sigma_1 E}] - N_2[1 - e^{\sigma_2 E}])}{(N_2\sigma_2 + N_1\sigma_1)E} \quad (6)$$

where TE_l and TE_c are the TEs for the linear electron flow and that for the cyclic electron flow in PSI, respectively. N_2 and N_1 are the numbers of reaction centers of PSII and PSI, respectively, σ_2 and σ_1 are the optical cross-sections of the photosynthetic units 2 and 1, respectively, and E is the flash energy flux. The factor 2 enters because the linear system requires two excitations. One should note that our assumption on the cyclic electron flow around PSI requires that $N_1\,(1 - e^{-\sigma_1 E}) > N_2\,(1 - e^{-\sigma_2 E})$. If these terms are equal, there is no cyclic electron flow. One can even extrapolate the assumption that, if the first term is smaller than the second, there would be a cyclic flow in PSII rather than in PSI, and these terms in Equation 6 should be exchanged. We assume an electron from PSII always finds an acceptor PSI. If not, a factor must be added to allow for this loss. If the σs of PSI and PSII are the same, an average TE is measured, i.e.

$$TE = TE_{max}^{lin,c}(1 - e^{-\sigma E})/\sigma E \quad (7a)$$

where

$$TE_{max}^{lin,c} = (2TE_{lin}N_2 + TE_c[N_1 - N_2])/(N_2 + N_1) \quad (7b)$$

Analysis of TE as a Summation of PSII and PSI

For the case of isolated or inhibited systems, the absorbed light energy is trapped separately by the two photosystems.

The TE as a function of flash energy can be rewritten from Equation 6:

$$TE = \frac{TE_{II}N_2\,(1 - e^{-\sigma_2 E}) + TE_I N_1\,(1 - e^{-\sigma_1 E})}{(N_2\sigma_2 + N_1\sigma_1)E} \quad (8)$$

where TE_{II} and TE_I are the TEs for PSII and PSI, respectively. If $\sigma_1 = \sigma_2 = \sigma$, an average TE is measured, i.e.

$$TE = TE_{\max}I,\ II\ (1 - e^{-\sigma E})/\sigma E \quad (9a)$$

where

$$TE_{\max}I,\ II = (TE_{II}N_2 + TE_I N_1)/(N_2 + N_1) \quad (9b)$$

One should note that Equations 7a and 9a are similar except that $TE_{\max}{}^{lin,c}$ and $TE_{\max}I,\ II$ are different.

The above equations allow the use of all the data to solve for the TEs themselves, which are the limits at infinitely weak flashes. The corresponding treatment of modulated light photoacoustic data would be to extrapolate measured values as an appropriate function of modulated light intensity to zero intensity. This procedure is required to obtain accurate values of TE. The above equations contain up to five independent parameters, and our acoustic data cannot provide all of them. Thus, the ratio of PSII to PSI and the optical cross-sections of the two units are taken from our recent work on *Chlorella* (19). The standard parameters referred to later are: $N_2/N_1 = 0.5$; $\sigma_2{}^{695} = 5 \times 10^{-15}$ cm^{-2}; $\sigma_1{}^{695} = 3 \times 10^{-14}$ cm^{-2}; $\sigma_2{}^{655} = \sigma_1{}^{655} = 3 \times 10^{-14}$ cm^{-2}. This reduces the number of independent variables to two or one, the TEs alone.

RESULTS

Figure 1 shows four integrated photoacoustic signals for *Chlorella* obtained in the dark (trace DK) and in the presence of continuous background light (trace LT). The acoustic signal shows a maximum at approximately 8 ms. Before 2 ms, it is caused by the sound waves formed on pulse heating the sample surface and, thus, does not provide an accurate measurement of heat in the bulk of the sample. The rise time is partly determined by the thermal conductivity in the sample and partly by the cell and microphone. The decay time is determined mostly by thermal loss into the sample and in part by the microphone itself (28). The small slow decrease or increase in the ratio between 2 and 20 ms is most likely caused by a baseline drift of the integrated signal. After 20 ms, the low signal to noise ratio and the drift prevent measurement of an accurate TE via the ratio of signals.

TE of Cyclic PSI

The TE of PSI was determined by excitation of intact *Chlorella* at 695 nm. At this wavelength, σ_1 is six times larger than σ_2 and $N_2/N_1 = 0.5$; therefore, 92% of the photons are trapped by PSI. In addition, the absorption in vivo is the same as that at 655 nm, in which both photosystems are excited. This choice of constant in vivo absorption helps compensate for internal light scatter and heterogeneous absorption effects (19). Figure 2 shows a plot of thermal efficiency as a function of incident laser flash energy for *Chlorella*. The solid curve is the theoretical cumulative one-hit Poisson saturation function (Eq. 6) using standard parameters. This reduces the number of unknowns to two, and the fit by least squares gives 38 ± 2% or 0.68 ± 0.04 eV/hv for TE_c and 47 ± 9% in TE_{lin} (Table Ia). Because the shape and the position of the curve on the absolute energy axis are fixed by totally different experiments (19), the overall fit of these data (Figs. 2 and 3) is very satisfying. The energy storage in linear electron transfer cannot be obtained accurately because only 8% of the photons are trapped by PSII. On the other hand, the TE for cyclic electron transfer in PSI is well defined. The data obtained at the slow flash rate were fit to Equation 8 because PSI and PSII are isolated when pulsed at 60 s per flash (see "Discussion"). The TE_I so obtained is the same value as TE_c obtained at the fast flash rate (Table Ia).

The TE of PSI was also determined as a function of flash energy at 695 nm with 1 μM DCMU-inhibited *Chlorella* (Fig.

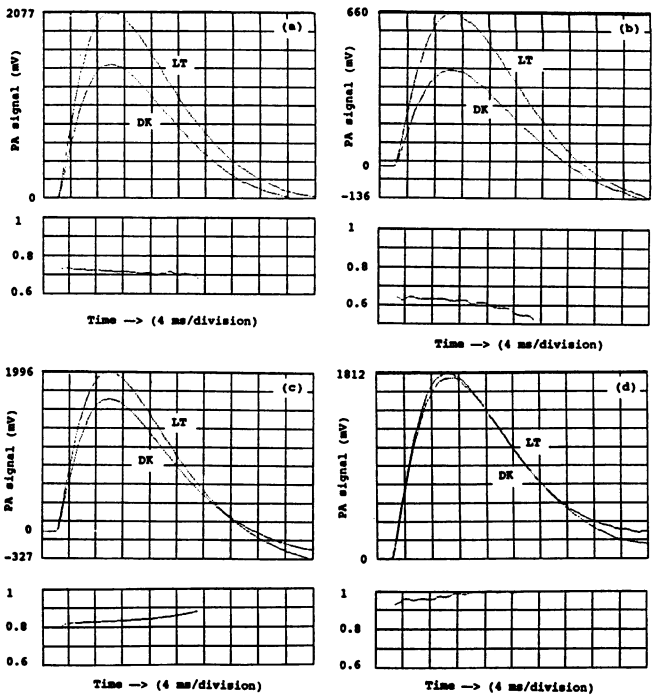

Figure 1. Top part of each panel, An integrated photoacoustic (PA) signal for *Chlorella* in the dark (trace DK, light intensity [400–700 nm]: <5 × 10^{11} quanta cm^{-2} s^{-1}) and in the presence of continuous background light (trace LT, light intensity [400–700 nm]: approximately 2 × 10^{16} quanta cm^{-2} s^{-1}). The excitation wavelength is 655 nm with flash intervals of 60 s in the dark and 0.35 s in the presence of background light. Bottom part of each panel, The plot of the ratio of acoustic signals produced in the dark and in the presence of background light. This ratio varies by ±3% from 2 to 20 ms. a, Flash energy of approximately 2 × 10^{13} quanta cm^{-2} pulse^{-1}, which excites approximately 30% of the units. b, Flash energy of approximately 2 × 10^{13} quanta cm^{-2} pulse^{-1}, which excites approximately 30% of the units in the presence of 1 μM DCMU. c, Flash energy of approximately 8 × 10^{13} quanta cm^{-2} pulse^{-1}, which excites approximately 60% of the units. d, Control with flash energy of approximately 2.5 × 10^{13} quanta cm^{-2} pulse^{-1}, sample was heated at 60°C for 10 min. The flash interval for this sample was 0.35 s in the dark rather than 60 s.

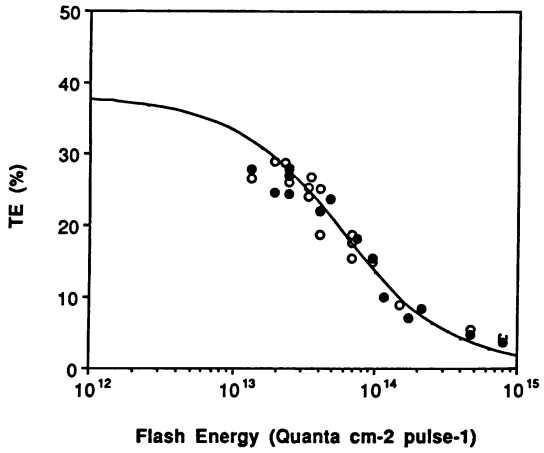

Figure 2. Plots of TE as a function of incident flash energy at 695 nm for *Chlorella*. The data were taken at approximately 8 ms, which is the maximum of the acoustic wave following a 1-μs flash. Each point is an average of 20 flashes with flash intervals of 0.35 s in the dark and 0.35 s in the presence of background light (light intensity [400–700 nm]: approximately 2×10^{16} quanta cm^{-1} s^{-1}). The TE at each flash energy was calculated from Equation 4b without correction for fluorescence. The solid curve is the cumulative one-hit Poisson saturation function (Eq. 6) using $\sigma_2 = 5 \times 10^{-15}$ cm^2, $\sigma_1 = 3 \times 10^{-14}$ cm^2, and $N_2/N_1 = 0.5$, fit by minimizing least square errors. O, No additives; ●, with 1 μM DCMU.

2). The data show 38% or 0.68 eV/hv for TE_I upon either fast or slow flashes (Table Ia). This energy storage in PSI is the same as that obtained from the uninhibited samples.

TE of Linear Electron Flow

The TE of linear electron flow from PSII to PSI was determined by excitation of *Chlorella* at the fast flash rate at 655 nm. At this wavelength, $\sigma_1 = \sigma_2 = \sigma$ and $N_2/N_1 = 0.5$; therefore, 33% of the photons are trapped by PSII (19). Because linear electron flow from PSII to PSI occurs under these conditions, the plot of TE versus energy was fit to Equation 7a. The least squares fit gives 30 ± 1% or 0.56 ± 0.02 eV/hv for $TE_{max}^{lin,c}$. Because $TE_c = 0.68$ eV/hv, obtained from the experiment at 695 nm, the energy storage in linear electron flow, TE_{lin}, is 0.50 ± 0.03 eV/hv calculated from Equation 7b (Table Ib). In Equation 7b, the TEs in units of eV/hv have to be used instead of that in percentage because TE_c and $TE_{max}^{lin,c}$ are obtained from two different wavelengths, 695 and 655 nm.

TE of Isolated PSII

The intact *Chlorella* samples were excited with 655 nm light at the slow flash rate. Figure 3 shows a plot of TE as a function of incident laser energy. The solid curve is the cumulative one-hit Poisson saturation function (Eq. 9a). Because PSII and PSI are isolated upon 60 s per flash and σs are the same, Equation 9a was used to fit the data. The least squares fit gives 43 ± 2% or 0.81 ± 0.04 eV/hv for $TE_{max}I, II$. A calculation from Equation 9b by using $TE_1 = 0.68$ eV/hv

Table I. *Summary of TEs of Chlorella vulgaris Excited at 695 and 655 nm*

TE_c and TE_{lin}, and TE_I and TE_{II} were calculated from Equations 6 and 8, respectively, with $\sigma_1 = 3 \times 10^{-14}$ cm^2 and $\sigma_2 = 5 \times 10^{-15}$ cm^2 at 695 nm. $TE_{max}^{lin,c}$ and $TE_{max}I, II$ were obtained by fitting the data to Equations 7a and 9a, respectively, with $\sigma = \sigma_1 = \sigma_2 = 3 \times 10^{-14}$ cm^2 at 655 nm. TE_I and TE_{II} were calculated from Equations 7b and 9b using $N_2/N_1 = 0.5$ and $TE_c = TE_I = 0.68$ eV/hv. All data were obtained by least square fit to ±2% error. Data in parentheses have large errors.

	0.35 s/Flash		60 s/Flash	
	%	eV	%	eV
(a) 695 nm				
No additives				
TE_c	38 ± 2	0.68 ± 0.04		
TE_{lin}	(47 ± 9)	(0.84 ± 0.16)		
TE_I			38 ± 2	0.68 ± 0.04
TE_{II}			(16 ± 16)	(0.29 ± 0.29)
With 1 μM DCMU				
TE_I	38 ± 3	0.68 ± 0.05	38 ± 2	0.68 ± 0.04
TE_{II}	(19 ± 19)	(0.34 ± 0.34)	(17 ± 17)	(0.30 ± 0.30)
(b) 655 nm				
No additives				
$TE_{max}^{lin,c}$	30 ± 1	0.56 ± 0.02		
TE_{lin}	27 ± 2	0.50 ± 0.03		
$TE_{max}I, II$			43 ± 2	0.81 ± 0.04
TE_{II}			56 ± 2	1.07 ± 0.05
With 1 μM DCMU				
$TE_{max}I, II$	33 ± 3	0.63 ± 0.06	43 ± 2	0.81 ± 0.04
TE_{II}	28 ± 2	0.53 ± 0.04	56 ± 2	1.07 ± 0.05

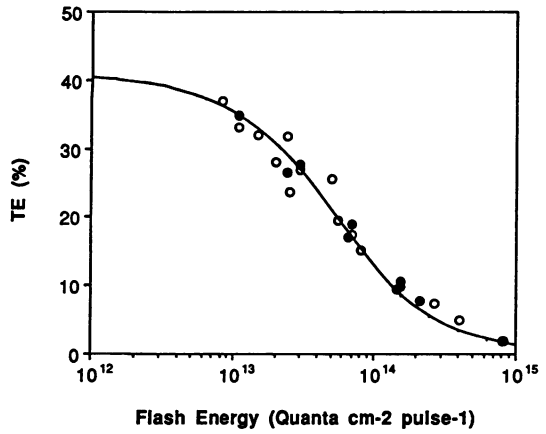

Figure 3. Plots of TE as a function of incident flash energy at 655 nm for *Chlorella*. The data were taken at approximately 8 ms, which is the maximum of the acoustic wave following a 1-μs flash. Each point is an average of 20 flashes with flash intervals of 60 s in the dark and 0.35 s in the presence of background light (light intensity [400–700 nm]: approximately 2×10^{16} quanta cm^{-1} s^{-1}). The fluorescence quantum yield at each flash energy (Y_f^d) was calculated from Equation 5 using $Y_f^{do} = 2.8\%$, $Y_f^l = 8.5\%$, and $\sigma = 3 \times 10^{-14}$ cm^2. The TE at each flash energy was calculated from Equation 4. The solid curve is the cumulative one-hit Poisson saturation function (Eq. 9a) using $\sigma = 3 \times 10^{-14}$ cm^2, fit by least square errors. O, No additives; ●, with 1 μM DCMU.

shows that the energy storage in PSII (TE_{II}) is 1.07 ± 0.05 eV/hv (Table Ib).

The energy storage of PSII in 1 μM DCMU-poisoned *Chlorella* was determined as a function of flash energy at the fast flash rate at 655 nm. The TE at each flash energy was calculated from Equation 4b using $Y_f^d = Y_f^l = 8.5\%$. The same fluorescence yield is used because the PSII reaction centers are essentially closed after the first few flashes. The energy storage in PSII is 0.53 ± 0.04 eV/hv calculated from Equation 9b (Table Ib). Data were also taken at the slow flash rate. The results are shown in Table Ib.

The TE was studied as a function of DCMU concentration at 655 nm at the fast flash rate with a flash energy of 2.5×10^{13} quanta cm^{-2} $pulse^{-1}$. The TE was 28% in the presence of 1 μM DCMU, which is sufficient to inhibit O_2 production in *Chlorella*. A 10-fold increase in the concentration of DCMU (10 μM) did not change this result, but the TE decreased to 15% at 50 μM of DCMU. A concentration of DCMU greater than 10 μM inhibits sites other than the $Q_A \rightarrow Q_B$ site (21). The evidence indicates a second site on the oxidizing side of PSII (12). Inhibition of storage of the positive charge and charge recombination with Q_A^- in <10 ms would cause a decrease in TE.

TE in the Presence of Other Inhibitors

Experiments were also carried out to determine the TE in the presence of other inhibitors, DBMIB and CCCP, at the two wavelengths with a single flash energy (Table II). In addition, the TE was determined in the simultaneous presence of two inhibitors, DCMU and DBMIB or DCMU and CCCP, respectively (Table II). The TE is not affected by mild heating at 50°C for 10 min. However, on heating the sample of *Chlorella* at 60°C for 10 min, the TE is 0 ± 2%. The difference of TE between slow and fast flash rates in the uninhibited sample (Table IIb) is less (5%) than in Table Ib (13%) because of the finite pulse energy (approximately 30% excitation). The data in Table I are extrapolated to zero excitation by the curve-fitting procedure.

TE as a Function of Background Light

Because the amount of light exciting the sample in the pulsed photoacoustic measurements (approximately 10^{13}-10^{15} quanta cm^{-2} $pulse^{-1}$) is many orders of magnitude less than that used in modulated light photoacoustics or fluorescence measurements (approximately 10^{18}-10^{21} quanta cm^{-2}), the effect of extended dark adaption and thus of induction processes was of concern. This is particularly so at the slow flash rate and lowest energy where a reaction center may be hit only once in 5 min. The energy storage in *Chlorella* was, therefore, studied as a function of continuous background light intensity (400–700 nm) in the presence and in the absence of DCMU at 695 nm (Fig. 4). Similar data were obtained at 655 nm (Fig. 5).

DISCUSSION

Our measurement of energy storage in *Chlorella* at various flash energies, wavelengths, and flash frequencies and in the presence of inhibitors allows us to determine the TEs of both linear and cyclic electron flows, the latter including PSI and possibly PSII. We will begin with cyclic flow about PSI and PSII and then consider linear flow because the results of the former are required for the latter.

Cyclic Electron Flow in PSI

The TE in PSI was determined by excitation of *Chlorella* at 695 nm. The constancy of the TE, 38% or 0.68 eV/hv (Table Ia) over a >100-fold range of flash frequency and in the

Table II. *Measured TE of Chlorella vulgaris in the Presence of Inhibitors*

Flash energy is 2.5×10^{13} quanta cm^{-2} at 695 and at 655 nm.

Conditions	60 s/Flash	0.35 s/Flash
	%	%
(a) 695 nm		
No inhibitor	28	27
10 μM DBMIB with 1 μM DCMU	27	25
10 μM CCCP with 1 μM DCMU	23	26
Heat at 50°C for 10 min	22	23
Heat at 60°C for 10 min		0 ± 1
(b) 655 nm		
No inhibitor	27	22
10 μM DBMIB with 1 μM DCMU	27	19
10 μM CCCP without DCMU	25	21
10 μM CCCP with 1 μM DCMU	27	21
Heat at 50°C for 10 min	24	26
Heat at 60°C for 10 min		0 ± 2

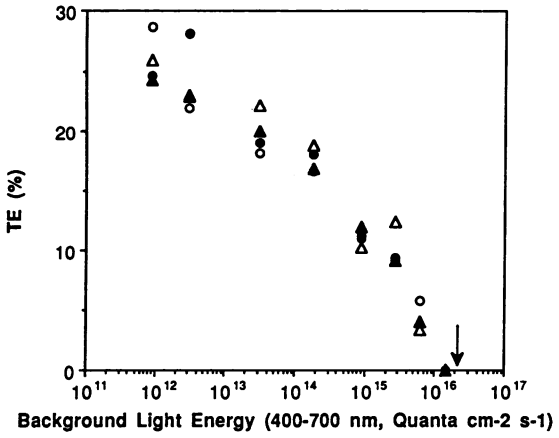

Figure 4. Plots of TE as a function of background light intensity (400–700 nm). Flash energy, which excites 30% of the units, is 2.5 × 10^{13} quanta cm^{-2} at 695 nm. Each point is an average of 20 flashes with flash separations of 60 and 0.35 s, respectively. The arrow indicates the intensity used for the continuous background light. O, No DCMU, 60 s per flash. ●, In the presence of 1 μM DCMU, 60 s per flash. Δ, No DCMU, 0.35 s per flash. ▲, 1 μM DCMU, 0.35 s per flash.

presence and absence of DCMU supports the contention that this is the energy stored in cyclic PSI. In addition, this result is the same whether estimated by linear-cyclic analysis (Eq. 6) or PSI-PSII analysis (Eq. 8) (Table Ia). However, this calculated TE is dependent on the ratio of reaction centers of PSII to those of PSI. If this ratio is increased from 0.5 to 1.0, the calculated energy storage of cyclic PSI at either flash rate would only decrease to 34 ± 2% or 0.61 ± 0.04 eV/hv. This equal ratio of PSII and PSI reaction centers was found only in *Chlorella* grown under extremes of irradiance (19).

The energy storage of 0.68 eV/hv in cyclic PSI is stored as intermediates whose lifetimes are greater than 20 ms. The lifetime of P700 is <200 μs (17) under single-flash conditions. Only under saturating light conditions is the lifetime of P700 approximately 150 ms (29). Hence, this intermediate is not measured by our photoacoustics. The lifetime of the FNR-Fd complex is a few ms in *Chlorella* (5) or in spinach thylakoids (18) with E_m° of −0.51 V (3, 31). The lifetime of Cyt b_6/f is not known (16). Its redox potential varies from 0 to 0.36 V (14).

If under our conditions the reduced FNR-Fd and the oxidized Cyt b_6/f complex have lifetimes of >20 ms, then the measured energy storage of 0.68 eV/hv can be assigned to the difference in their redox energy, 0.5 to 0.85 eV. If not, then the energy is stored as an ion and proton gradient and/or in protein conformation changes. The complex cycle, which involves quinones and Cyt b_6/f, is supposed to pump two protons per electron transferred (34). The amount of energy stored depends on the pH gradient and will be approximately 0.2 eV per proton for a 3 pH unit gradient. Because we measure an energy storage of 0.68 eV, there is no thermodynamic difficulty with pumping two or three protons given a suitable mechanism. It is interesting that an estimate of the maximal working free energy change in PSI is 0.7 eV (1). This conclusion is based on the lack of observing delayed luminescence from PSI. If the luminescence yield from PSI differs from that of PSII, the estimate will change accordingly. Our result indicates that the yields are similar or PSI has a lower yield.

A conflicting result is the lack of inhibition by DBMIB, which is claimed to inhibit both linear and cyclic electron flows. However, the claim of inhibition of cyclic flow is based on synthetic systems utilizing artificially enhanced cycling, and only certain of these systems, catalyzed by Fd, menadione, thymoquinone, and duroquinone, are inhibited, and not those catalyzed by diaminodurene and methylphenazonium methosulfate (33). Herbert et al. (20) observed a partial inhibition of a cyclic PSI, measured by modulated light photoacoustics using a much higher concentration (100 μM) of DBMIB in which other inhibitory effects may enter. The light intensity they used is also much higher than that used in our experiments. Possibly, a certain light flux is required, as with DCMU, to observe the inhibition. The same explanation could apply to the CCCP experiment, in which the effect is small and is close to our experimental limit. It is possible that very little proton gradient exists at the very low average light input in the present experiments.

Linear Electron Flow

The overall TE ($TE_{max}^{lin,c}$) at the fast flash rate at 655 nm is 30 ± 1% or 0.56 ± 0.02 eV/hv (Table Ib), close to the value found for *Ulva* by Herbert et al. (20) using modulated light photoacoustics. With the fast flash rate, O_2 and NADPH are the products at 20 ms; therefore, the result can be decomposed into linear and cyclic flow TEs (Eq. 7b). Assuming the previously obtained value of 0.68 eV/hv for cyclic flow in PSI, the energy storage for linear flow is 0.50 ± 0.03 eV/hv.

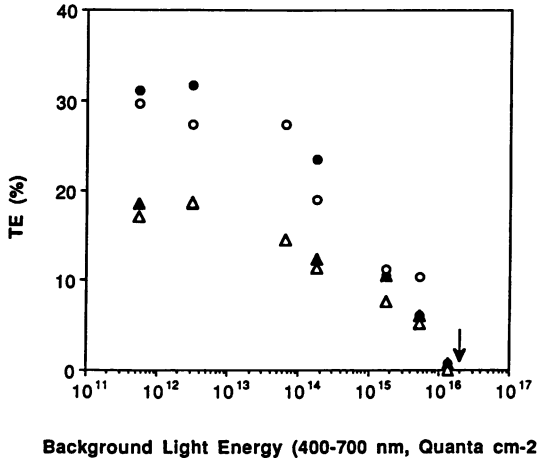

Figure 5. Plots of TE as a function of background light intensity (400–700 nm). Flash energy, which excites 30% of the units, is 2.5 × 10^{13} quanta cm^{-2} at 655 nm. Each point is an average of 20 flashes with flash separations of 60 and 0.35 s, respectively. The arrow indicates the intensity used for the continuous background light. O, No DCMU, 60 s per flash. ●, In the presence of 1 μM DCMU, 60 s per flash. Δ, No DCMU, 0.35 s per flash. ▲, 1 μM DCMU, 0.35 s per flash.

This is close to that expected for linear flow of an electron from S-state (0.9 eV) (6) to $NADP^+$ (−0.32 eV) (2), 0.61 eV/hv.

The 20% smaller value observed may be the result of the following. (a) The use of standard potentials can cause an error of approximately ± 0.1 eV because of different concentrations (100-fold) of reactants and/or pH (±2 units) effects. (b) A possible explanation of the discrepancy may be entropic effects mentioned earlier. One is comparing free energies of the products with the enthalpy measurements of photoacoustics; thus, the difference is a direct measure of the entropy changes in the system. (c) Another explanation is that, contrary to the assumption for Equations 6 and 7, a and b, not all PSII electrons find a PSI or vice versa. A loss of about 20% of the flow would explain the discrepancy.

Isolated PSII

At the slow flash rate with intact *Chlorella*, the overall TE with 655 nm of light increases to 43 ± 2%, in comparison to 30% at the fast flash rate. At the slow flash rate, the higher S-states are largely lost between excitations. The half-life of the S_2-state is 20 s and that of the S_3-state is 5 s in *Chlorella* (22). On the acceptor side, the electron transfer from Q_A to Q_B occurs in 200 μs (7). Q_B^- has a long lifetime of a few seconds (32). Thus, at the time of 10 ms and a reaction center II hit rate of about one in 300 s, an energy of 1.03 eV is calculated, corresponding to the redox energy between the S_2-state (0.9 eV) (6) and Q_B^- (0.13 eV) (15). The energy storage in PSII is 1.07 eV/hv calculated from Equation 9b using a TE_l of 0.68 eV/hv (Table Ib). The system thus behaves as an isolated preparation, in which higher TEs are expected because only partial reactions are observed.

Similar observations can be found in the literature with regard to isolated subsystems. Camm et al. (9) using 600 to 640 nm of light found an energy storage of 34% in PSII particles but only 24% in broken chloroplasts from barley at approximately 14 ms. Carpentier et al. (13), using 690 nm of light obtained a TE of 42% in PSII particles from spinach at approximately 14 ms. Both groups used modulated light photoacoustics. Nitsch et al. (30), using pulsed light at 677 nm but an essentially single-time point (2 μs) resonant detector, found a TE of 85 ± 8% in PSI and 65 ± 7% in PSII particles from the cyanobacterium *Synechococcus* sp. The higher percentages at this short time correspond to more energetic species such as $P680^+$ and Q_A^-. The above experiments also depend on the quality of the preparation. The advantage of our method is that it allows the study of isolated systems in vivo.

Cyclic Electron Flow in PSII

A striking result is that DCMU does not lower the overall TE at 655 nm (30 versus 33 or 43 versus 43%) (Table Ib). Any change at 1 μM DCMU is within the error at 655 nm using either fast or slow flash rates. One complication in these experiments is the reoxidation of Q_A^- in the presence of DCMU. In *Chlorella*, the dark decay of increased fluorescence has a lifetime (nonexponential) of approximately 0.7 s (4). Thus, at the slow flash rate, no effect of DCMU is expected. The energy is simply stored in Q_A^- and the S_2-state with a calculated redox energy difference of 0.92 eV (6). At the fast flash rate, the mean time between hits of a given reaction center is 1 to 3 s at the lowest flash energy. Thus, about 50 to 70% of the reaction centers may be returned to the ground state between flashes. These centers remain in the "first hit," i.e. high TE state. This could explain the observation that the energy stored in PSII in the presence of DCMU decreases by only a factor of 2, 0.53 versus 1.07 eV/hv (Table Ib).

However, addition of background light should "compensate" for the slow flash rate and cause a decrease in TE when the overall excitation rate approaches 1 s^{-1}. This is expected to occur at the background light intensity of approximately 10^{13} quanta cm^{-2} s^{-1}, given that the turnover time of the linear system is approximately 10 ms at saturation. No such effect is observed (Fig. 5). Note that these results with DCMU cannot be explained by an efficient "spillover" mechanism by which energy absorbed by the PSII antennae but not used at reaction center II is transferred to PSI. Were that the case, the apparent cross-section of the measurement at 655 nm would double, and this is not observed (Fig. 3).

We conclude that we have some evidence that at 20 ms energy storage of 0.53 eV/hV occurs in a cyclic PSII. The high potential Cyt b_{559} is a feasible candidate for this energy storage if its turnover time is in fact ≤0.1 s (35).

The continuous background light saturation curves with 695 and 655 nm excitation show that the TE is not "rescued" or "induced" by the presence of a small amount of continuous light (Figs. 4 and 5). These results indicate that the very low light level of our pulsed measurements does not require a supplement (induction) by weak background light. The higher TE with 655 nm at 60 s per flash than that at 0.35 s per flash shows that the higher energy is stored in charge-separated intermediates rather than in final products as discussed above.

In conclusion, the energy storage in cyclic PSI in intact *Chlorella* has been determined to be 0.68 eV/hv and that for linear electron flow to be 0.50 eV/hv. The small DCMU effect on PSII TE may indicate a significant cyclic electron flow in PSII.

ACKNOWLEDGMENTS

The authors wish to thank Irene Zielinski-Large for growing *Chlorella* and for technical assistance, The Knowles Co. for providing microphones, Drs. Nancy Greenbaum, Jeffrey Hind, and Paul Falkowski for useful discussions, and Dr. Shmuel Malkin for critically reading the manuscript.

LITERATURE CITED

1. **Arcelay AR, Ross RT, Ezzeddine BM** (1988) Photosystem I generates a free-energy change of 0.7 electron volts or less. Biochim Biophys Acta **936:** 199–207
2. **Arnon DI** (1969) Role of ferredoxin in photosynthesis. Naturwissen **56:** 295–305
3. **Batie C, Kamin H** (1981) The relation of pH and oxidation-reduction potential to the association state of the ferredoxin: ferredoxin:$NADP^+$ reductase complex. J Biol Chem **256:** 7756–7763
4. **Bennoun P** (1970) Reoxydation du quencher de fluorescence "Q" en presence de 3-(3,4-dichlorophenyl)-I,I-dimethylurea. Biochim Biophys Acta **216:** 357–363

5. **Bouges-Bocquet B** (1978) Absorption changes from 437 nm to 530 nm in *Chlorella pyrenoidosa* under flash excitation. FEBS Lett **85:** 340–344
6. **Bouges-Bocquet B** (1980) Kinetic models for the electron donors of photosystem II of photosynthesis. Biochim Biophys Acta **594:** 85–103
7. **Bowes J, Crofts AR** (1980) Binary oscillations in the rate of reoxidation of the primary acceptor of photosystem II. Biochim Biophys Acta **590:** 373–384
8. **Bults G, Horwitz BA, Malkin S, Cahen D** (1982) Photoacoustic measurements of photosynthetic activities in whole leaves photochemistry and gas exchange. Biochim Biophys Acta **679:** 452–465
9. **Camm EL, Popovic R, Lorrain L, LeBlanc RM, Fragata M** (1988) Photoacoustic characterization of energy storage of photosystem 2 core-enriched particles from barley isolated with the octyl-β-D-glucopyranoside detergent. Photosynthetica **22:** 27–32
10. **Canaani O, Malkin S** (1984) Physiological adaptation to a newly observed low light intensity state in intact leaves, resulting in extreme imbalance in excitation energy distribution between the two photosystems. Biochim Biophys Acta **766:** 525–532
11. **Canaani O, Malkin S, Mauzerall D** (1988) Pulsed photoacoustic detection of flash-induced oxygen evolution from intact leaves and its oscillations. Proc Natl Acad Sci USA **85:** 4725–4729
12. **Carpentier R, Fuerst EP, Nakatani HY, Arntzen CJ** (1985) A second site for herbicide action in photosystem II. Biochim Biophys Acta **808:** 293–299
13. **Carpentier R, Leblanc R, Mimeault M** (1989) Photoacoustic detection of photosynthetic energy storage in photosystem II submembrane fractions. Biochim Biophys Acta **975:** 370–376
14. **Cramer W** (1977) Cytochromes. *In* A Trebst, M Avron, eds, Photosynthesis, Vol I: Photosynthetic Electron Transport and Photophosphorylation. Springer-Verlag, Berlin, FRG, pp 227–237
15. **Cramer W, Crofts AR** (1982) Electron and proton transport. *In* Govindjee, ed, Photosynthesis, Vol I. Academic Press, New York, pp 387–467
16. **Crowther D, Hind G** (1980) Partial characterization of cyclic electron transport in intact chloroplasts. Arch Biochem Biophys **204:** 568–577
17. **DeLosme R, Zickler A, Joliot P** (1978) Turnover kinetics of photosystem I measured by the electrochromic effect in *Chlorella*. Biochim Biophys Acta **504:** 165–174
18. **Garab G, Hong Y, Coughlan SJ, Matthijs HCP, Hind G** (1990) Absorbance transients of ferredoxin: $NADP^+$ reductase in isolated thylakoid membranes. *In* M Baltscheffsky, ed, Current Research in Photosynthesis, Vol II. Kluwer Academic Publishers, Dordrecht, The Netherlands, pp 667–670
19. **Greenbaum NL, Mauzerall D** (1991) Effect of irradiance level on distribution of chlorophylls between PSII and PSI as determined from optical cross-sections. Biochim Biophys Acta **1057:** 195–207
20. **Herbert SK, Fork D, Malkin S** (1990) Photoacoustic measurements *in vivo* of energy storage by cyclic electron flow in algae and higher plants. Plant Physiol **94:** 926–934
21. **Izawa S, Good NE** (1972) Inhibition of photosynthetic electron transport and photophosphorylation. Methods Enzymol **24:** 355–377
22. **Joliot P, Joliot A, Bouges B, Barbieri G** (1971) Studies of system II photocenters by comparative measurements of luminescence, fluorescence, and oxygen emission. Photochem Photobiol **14:** 287–305
23. **Latimer P, Bannister T, Rabinowitch EI** (1957) The absolute quantum yields of fluorescence of photosynthetically active pigments (papers presented at the Gatlinburg Conference, 1955). *In* H Gaffron, ed, Research in Photosynthesis. Interscience, New York, pp 107–112
24. **Ley AC, Mauzerall, D** (1982) Absolute absorption cross sections for photosystem II and the minimum quantum requirement for photosynthesis in *Chlorella vulgaris*. Biochim Biophys Acta **680:** 95–106
25. **Ley AC, Mauzerall D** (1986) The extent of energy transfer among photosystem II reaction centers in *Chlorella*. Biochim Biophys Acta **850:** 234–248
26. **Malkin S, Cahen D** (1979) Photoacoustic spectroscopy and radiant energy conversion: theory of the effect with special emphasis on photosynthesis. Photochem Photobiol **29:** 803–813
27. **Mauzerall D** (1980) Fluorescence and photosynthesis: gated detection and analysis of nanosecond pulse excitation. Adv Biol Med Phys **17:** 173–198
28. **Mauzerall D** (1990) Determination of oxygen emission and uptake in leaves by pulsed, time resolved photoacoustics. Plant Physiol **94:** 278–283
29. **Maxwell P, Biggins J** (1976) Role of cyclic electron transport in photosynthesis as measured by the photoinduced turnover of P_{700} *in vivo*. Biochemistry **15:** 3975–3981
30. **Nitsch C, Braslavsky S, Schatz G** (1988) Laser-induced optoacoustic calorimetry of primary processes in isolated photosystem I and photosystem II particles. Biochim Biophys Acta **934:** 201–212
31. **Pschorn R, Ruhle W, Wild A** (1988) Structure and function of ferredoxin-$NADP^+$-oxidoreductase. Photosynth Res **17:** 217–229
32. **Pulles M, Van Gorkom HJ, Willemsen G** (1976) Absorbance changes due to the charge-accumulating species in system 2 of photosynthesis. Biochim Biophys Acta **449:** 536–540
33. **Trebst A** (1980) Inhibitors in electron flow: tools for the functional and structural localization of carriers and energy conservation sites. Methods Enzymol **69:** 675–705
34. **Trumpower B** (1990) The protonmotive Q cycle. J Biol Chem **265:** 11409–11412
35. **Whitmarsh J, Cramer WA** (1977) Kinetics of the photoreduction of cytochrome *b*-559 by photosystem II in chloroplasts. Biochim Biophys Acta **460:** 280–289